($5.5\ e_0$ versus $12.3\ e_0$). The fact that q for the V2 channel, as measured through voltage sensitivity of activation, is underestimated shows that estimates of q obtained in this way must be interpreted carefully.

REFERENCES AND NOTES

1. A. L. Hodgkin and A. F. Huxley, *J. Physiol. (London)* **117**, 500 (1952).
2. M. Noda *et al.*, *Nature* **312**, 121 (1984).
3. W. Stühmer *et al.*, *ibid.* **339**, 597 (1989).
4. D. M. Papazian, L. C. Timpe, Y. N. Jan, L. Y. Jan, *ibid.* **349**, 305 (1991).
5. E. R. Liman, P. Hess, F. Weaver, G. Koren, *ibid.* **353**, 752 (1991).
6. K. McCormack *et al.*, *Proc. Natl. Acad. Sci. U.S.A.* **88**, 2931 (1991).
7. L. E. Iverson and B. Rudy, *J. Neurosci.* **10**, 2903 (1990).
8. Construction of inactivating WT and V2 *Shaker* 29-4 cDNA and in vitro synthesis of mRNA is described (*6*, 7). WT and V2 channels were made noninactivating by replacement of the Sac I–Nar I fragment from the *Shaker* 29-4 Bluescript (Stratagene) construct with complementary oligonucleotides that deleted amino acid residues 2 to 29. The constructs were sequenced to ensure that only the appropriate changes were introduced. *Xenopus laevis* oocytes were injected with WT or V2 mRNA (~3 ng) and patch-clamped 4 to 21 days later. Conventional oocyte macropatch techniques were used (*15*) with pipettes having a 3- to 10-μm diameter (0.5- to 2.0-megohm resistance) pulled from Kimax capillaries. Recordings were made from inside-out membrane patches at 21° to 23°C with an EPC-9 patch clamp (Heka Electronic, Lambrecht, Germany).
9. T. Hoshi, W. N. Zagotta, R. W. Aldrich, *Science* **250**, 533 (1990).
10. K. McCormack, J. W. Lin, L. E. Iverson, B. Rudy, *Biochem. Biophys. Res. Commun.* **171**, 1361 (1990).
11. G. A. Lopez *et al.*, *Neuron* **7**, 327 (1991).
12. W. Almers, *Rev. Physiol. Biochem. Pharmacol.* **82**, 96 (1978).
13. C. M. Armstrong and F. Bezanilla, *Nature* **242**, 459 (1973); R. D. Keynes and E. Rojas, *J. Physiol. (London)* **239**, 393 (1974); W. Nonner, E. Rojas, R. Stämpfli, *Pfluegers Arch.* **375**, 75 (1975).
14. H. Meves, *J. Physiol. (London)* **243**, 847 (1974).
15. W. Stühmer, F. Conti, M. Stocker, O. Pongs, S. H. Heinemann, *Pfluegers Arch.* **418**, 423 (1991).
16. For the subtraction of linear leakage currents in the gating-current recordings, alternating positive and negative 20-mV pulses were applied from −120 mV and the responses were subtracted and scaled appropriately to the test pulse. Artifacts resulting from charge movement during the −120- to −100-mV leak subtraction pulses were estimated and corrected (*15*). However, we were unable to correct for charge movement during the −120- to −140-mV pulses, which might have slightly distorted the initial phases of the gating currents. The "on" gating currents did not show a rising phase, as was reported in gating currents from another truncated, noninactivating *Shaker* channel (*18*). The origin of this discrepancy is unclear although it may involve differences in the recording technique (whole-oocyte versus patch recordings) or differences in the *Shaker* constructs used.
17. F. Bezanilla, M. M. White, R. E. Taylor, *Nature* **296**, 657 (1982); M. W. White and F. Bezanilla, *J. Gen. Physiol.* **85**, 539 (1985); S. Spires and T. Begenisich, *ibid.* **93**, 263 (1989).
18. F. Bezanilla, E. Perozo, D. M. Papazian, E. Stefani, *Science* **254**, 679 (1991).
19. The difference in the decay rates of the V2 and WT "off" gating currents is probably related to the fact that deactivation in V2 channels occurs much more rapidly than in WT channels. The time constants of decay for "off" gating currents and ionic tail currents following a large depolarization were both ~5 ms for the WT channel and ~0.75 and 0.20 ms, respectively, for the V2 channel.
20. F. J. Sigworth, *J. Physiol. (London)* **307**, 97 (1980).
21. As a check for the reliability of the fluctuation analysis results, estimates for single channel current (i) and p_o (1.5 ± 0.2 pA and 0.79 ± 0.08 for WT at +80 mV, n = 8; 1.3 ± 0.2 pA and 0.68 ± 0.08 for V2 at +160 mV, n = 9) were compared with and found to be very close to those obtained from parallel single channel recordings (1.7 pA, 0.80, 1.5 pA, and 0.55, respectively). However, the V2 channel displays variable kinetics and multiple conductance levels, with i at +160 mV most commonly ~1.5 or ~3 pA. To check the validity of the fluctuation analysis results for the V2 channels more directly, we analyzed recordings from patches where there was a known number of V2 channels. In three patches containing one, one, and three channels, fluctuation analysis of the ensembles (280, 450, and 149 records, respectively) yielded N values of 1.0, 1.5, and 2.8. These results and theoretical considerations suggest that systematic errors in the fluctuation analysis, if present, would tend toward overestimation of N and thus underestimation of q for the V2 channel.
22. TEA^+ might be expected to interfere with the "on" charge movement, as (unlike CTx) it appeared to abolish the "off" charge movement (Fig. 3C) at large depolarizations, as reported previously for truncated *Shaker* H4 (*18*). However, TEA^+ added to the bath did not change the time course and amplitude of "on" currents in other patches that contained WT or V2 channels already blocked by CTx. Moreover, measurements of V2 gating currents made without ionic currents blocked yielded similar estimates of q (12.6 ± 0.3 e_0, n = 3), as did two additional experiments where tetramethylammonium ion, which does not block the "off" currents, was used in the bath solution instead of TEA^+ (12.2 and 11.2 e_0 for WT and V2, respectively).
23. L. C. Timpe *et al.*, *Neuron* **1**, 659 (1988); L. E. Iverson *et al.*, *Proc. Natl. Acad. Sci. U.S.A.* **85**, 5723 (1988).
24. W. N. Zagotta and R. W. Aldrich, *J. Gen. Physiol.* **95**, 29 (1990).
25. G. Koren *et al.*, *Neuron* **2**, 39 (1990).
26. For both WT and V2 channels, a long delay precedes the rise of ionic currents following a step depolarization (Fig. 1B). To fit the time course of the currents, at least 12 closed states were required for a linear scheme to account for the delay.
27. C. L. Schauf and M. A. Chuman, in *Ion Channels in Neural Membranes*, J. M. Ritchie, D. R. Keynes, L. Bolis, Eds. (Liss, New York, 1986), p. 3.
28. F. Conti, I. Inoue, F. Kukita, W. Stühmer, *Eur. Biophys. J.* **11**, 137 (1984).
29. Abbreviations for the amino acid residues are: A, Ala; E, Glu; F, Phe; G, Gly; H, His; I, Ile; K, Lys; L, Leu; M, Met; Q, Gln; R, Arg; S, Ser; T, Thr; and V, Val.
30. A. Kamb *et al.*, *Neuron* **1**, 421 (1988).
31. K. Lucchesi, A. Ravindran, H. Young, E. Moczydlowski, *J. Membr. Biol.* **109**, 269 (1989).
32. Alternative Q estimates that would be insensitive to the uncorrected charge movement between −120 and −140 mV were obtained by fitting the "on" gating currents to one or two exponentials plus a constant term and taking Q to be the integral of the exponential function. The resulting values were within ~10% of those obtained by numerical integration. Estimates of q obtained by fitting the "on" gating currents were an average of 8% larger than those obtained by numerically integrating the currents.

33. We thank L. Iverson for making some of the cRNA; T. McCormack for sequence verification of noninactivating deletion constructs; L. Lin for oocyte preparation; E. Moczydlowski for CTx; S. H. Heinemann for helpful discussions; and W. K. Chandler and T. Woolf for comments on the manuscript. Supported by NIH grants to F.J.S., M.A.T., and L. Iverson.

16 October 1991; accepted 14 January 1992

Tumor Necrosis Factor–α Activates the Sphingomyelin Signal Transduction Pathway in a Cell-Free System

KENNETH A. DRESSLER, SHALINI MATHIAS, RICHARD N. KOLESNICK*

The mechanism of tumor necrosis factor (TNF)–α signaling is unknown. TNF-α signaling may involve sphingomyelin hydrolysis to ceramide by a sphingomyelinase and stimulation of a ceramide-activated protein kinase. In a cell-free system, TNF-α induced a rapid reduction in membrane sphingomyelin content and a quantitative elevation in ceramide concentrations. Ceramide-activated protein kinase activity also increased. Kinase activation was mimicked by addition of sphingomyelinase but not by phospholipases A_2, C, or D. Reconstitution of this cascade in a cell-free system demonstrates tight coupling to the receptor, suggesting this is a signal transduction pathway for TNF-α.

SPHINGOMYELIN CAN BE METABOlized to generate molecules that have various functions within the cell (*1–5, 6*). Ceramide, which is generated by sphingomyelinase action, can be deacylated to sphingoid bases (*1, 2*), which are potential inhibitors of protein kinase C (*3*) or phosphorylated to ceramide 1-phosphate (*4*) by a ceramide kinase (*5*). Ceramide appears to have bioeffector properties (*7, 8*). Cell-permeable ceramide analogs stimulate monocytic differentiation of human leukemia (HL-60) cells (*7*) and the phosphorylation of the epidermal growth factor receptor (EGFR) at Thr^{669} in A431 human epidermoid carcinoma cells (*8*). TNF-α activates a neutral sphingomyelinase to generate ceramide in HL-60 cells, and it was postulated that this initiated TNF-α action (*9*). We defined a ceramide-activated protein kinase with a synthetic peptide derived from the amino acid sequence surrounding Thr^{669} of the EGFR (residues 663 to 681) (*10*). Kinase activity was membrane-associated, Mg^{2+}-dependent, and activated by natural or synthetic ceramide in a concentration- and time-dependent manner. This ceramide-

Laboratory of Signal Transduction, Sloan-Kettering Institute, Memorial Sloan-Kettering Cancer Center, New York, NY 10021.

*To whom correspondence should be addressed.

activated protein kinase activity was rapidly increased in membranes derived from HL-60 cells treated with TNF-α. The present studies were undertaken to evaluate coupling of this sphingomyelin pathway to stimulation of the TNF receptor in a cell-free system.

The binding of TNF-α to its receptor is detectable within 2 min and maximal by 5 to 10 min at 4°C in membranes derived from HL-60 cells (*11*). Therefore, supernates from HL-60 cells, collected after a low-speed centrifugation to remove nuclei, were first incubated with TNF-α for 5 min at 4°C to allow the formation of TNF–receptor complexes. Thereafter, reactions were initiated by warming supernates to 22°C in a reaction mixture containing adenosine triphosphate (ATP) and Mg^{2+} at pH 7.4. These conditions were adopted to allow for activation of neutral sphingomyelinase (*1, 12*). Under these conditions, TNF-α induced a time- and concentration-dependent reduction in sphingomyelin content (Fig. 1A). The effect of TNF-α was evident at 1 min and maximal by 7.5 min. Sphingomyelin concentrations decreased 27% from a control concentration of 10.4 ± 0.5 (mean ± SEM) to 7.6 ± 0.2 nmol per milligram (nmol mg^{-1}) of supernate protein ($P < 0.001$). In contrast, the concentration of sphingomyelin in control incubations did not change. Concentrations of TNF-α of 300 pM were effective, with a maximal effect at 3 nM TNF-α [effective dose (ED_{50}) ≈ 500 pM]. Under the same conditions, ceramide increased quantitatively from 1.8 ± 0.3 to 4.0 ± 0.5 nmol mg^{-1} (Fig. 1B). This effect was detectable at 1 min ($P < 0.001$) and maximal by 7.5 min. Thus, 2.8 nmol of sphingomyelin per milligram of supernate protein were lost for each 2.2 nmol of ceramide per milligram of supernate protein that was generated. Similar kinetics of sphingomyelin degradation and ceramide generation were determined in intact HL-60 cells ($n = 3$), confirming previous studies (*9*). Other choline-containing lipids, including phosphatidylcholine, lysophosphatidylcholine, and sphingosylphosphorylcholine (*1*), and 1,2-diacylglycerol were not affected by TNF-α. Thus, TNF-α activated a neutral sphingomyelinase in a cell-free system, which resulted in the generation of the potential second messenger ceramide.

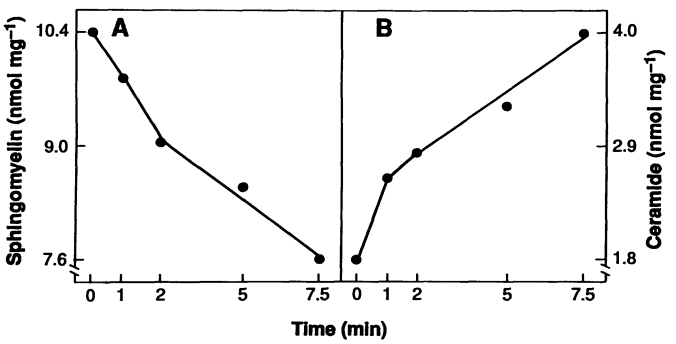

Fig. 1. TNF-α effects on sphingomyelin (**A**) and ceramide (**B**) concentrations in a cell-free system. HL-60 cells were grown in RPMI 1640 medium supplemented with 10% bovine calf serum and amino acids (*4*). To measure sphingomyelin, we resuspended cells (1×10^6 ml^{-1}), labeled for 48 hours in medium with [^{3}H]choline (1 μCi ml^{-1}) (*29*), in serum-free medium containing bovine insulin (5 μg ml^{-1}) and human transferrin (5 μg ml^{-1}). After 3 hours, cells were resuspended (150×10^6 ml^{-1}) in homogenization buffer (50 mM NaF, 5 mM EGTA, and 25 mM Hepes, pH 7.4), disrupted at 4°C with 150 strokes of a tight-fitting Dounce homogenizer (Fisher Scientific, Pittsburgh, Pennsylvania), and centrifuged for 5 min (500*g*). The nuclei-free supernate was first incubated for 5 min at 4°C with 30 nM human TNF-α (Genentech, South San Francisco, California) or diluent (50 mM Hepes, pH 7.4). At time zero, 15 μl of supernate (112 μg per incubation) were added to a reaction mixture containing 30 μl of 25 mM Hepes, pH 7.4, 30 μl of 750 μM ATP, and 75 μl of reaction buffer (50 mM Hepes, pH 7.4, and 20 mM $MgCl_2$) at 22°C. The reaction was terminated with $CHCl_3$:CH_3OH:HCl (100:100:1; v/v/v) (*4, 5, 13*) and 150 μl of balanced salt solution (135 mM NaCl, 4.5 mM KCl, 1.5 mM $CaCl_2$, 0.5 mM $MgCl_2$, 5.6 mM glucose, and 10 mM Hepes, pH 7.2) containing 20 mM EDTA. Lipids in the organic phase extract were subjected to alkaline methanolysis to remove glycerophospholipids (*4*). Sphingomyelin recovery in the nuclei-free supernate was 93% of that in intact cells. A measure of 10^6 cell equivalents of supernate contained 50 μg of protein. Sphingomyelin was resolved by thin-layer chromatography (TLC) with $CHCl_3$:CH_3OH:CH_3COOH:H_2O (25:15:4:1.5) as solvent, identified by iodine vapor staining, and quantified by liquid scintillation spectrometry (*1, 7, 28*). Ceramide was quantified with the diacylglycerol kinase reaction (*4, 29*). Values (mean) are derived from triplicate determinations from one experiment representative of three similar studies for sphingomyelin and four similar studies for ceramide.

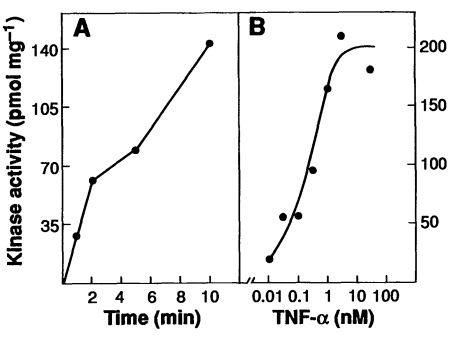

Fig. 2. Effect of TNF-α on ceramide-activated protein kinase activity. HL-60 cells were incubated in serum-free medium and homogenized (as in Fig. 1). After an initial incubation with TNF-α, 15 μl of nuclei-free supernate (112 μg per incubation) were added to a reaction mixture containing 30 μl of EGFR peptide (4 mg ml^{-1} in 25 mM Hepes, pH 7.4), 30 μl of [γ-^{32}P]ATP (750 μM, 4000 dpm $pmol^{-1}$), and 75 μl of reaction buffer (*10*). We terminated the reaction by adding 30 μl of 0.5 M ATP in 90% formic acid. Phosphorylated peptide was first run on a C_{18} Sep-Pak cartridge, then resolved by C_{18} reverse-phase HPLC (Waters, Milford, Massachusetts), with a linear gradient of acetonitrile. The peptide eluted at 30% acetonitrile, as we determined by monitoring Cerenkov radiation in 1-ml fractions. Background activity was subtracted from each point. (**A**) Kinetics of TNF-α (30 nM)–stimulated EGFR peptide phosphorylation. Values (mean) represent data from four experiments. (**B**) Concentration dependence of EGFR peptide phosphorylation at 5 min of stimulation with TNF-α (0.01 to 30 nM). Values (mean) represent data derived from duplicate points in two experiments. The SEM of the values in (A) was 18% and the mean range of values in (B) was 3%.

The effect of TNF-α on ceramide-activated protein kinase activity was assessed. Nuclei-free supernates contain ceramide-activated protein kinase activity that can phosphorylate EGFR peptide with a maximum velocity (V_{max}) of 50 to 100 pmol per minute per milligram (pmol min^{-1} mg^{-1}) of protein and a Michaelis constant (K_m) of 15 μM for ATP and 0.25 mg ml^{-1} for peptide (*10*). Ceramide (0.001 to 3 μM) enhances kinase activity to a maximum of twofold of control (*10*). TNF-α, which increased ceramide concentrations, similarly enhanced kinase activity in intact cells (*10*). For studies assessing the effect of TNF-α in broken cell preparations, nuclei-free supernates were incubated under conditions sufficient for stimulation of neutral sphingomyelinase in a reaction mixture that also contained EGFR peptide and γ-^{32}P-labeled ATP. Phosphorylated peptide was resolved by high-performance liquid chromatography (HPLC) and quantified by Cerenkov counting (*10*). Kinase activity was calculated from the specific activity of [γ-^{32}P]ATP and incorporation of ^{32}P into EGFR peptide. Background activity was subtracted from each point. TNF-α (30 nM) treatment enhanced kinase activity ($P < 0.001$) in a time-dependent manner (Fig. 2A). TNF-α stimulation of kinase activity was evident by 1 min and demonstrable for at least 10 min. If the initial incubation with TNF-α at 4°C was omitted and TNF was added directly to the reaction mixture at 22°C, the reaction was delayed. Under these conditions, enhancement of activity by TNF-α did not occur for 2 min, presumably until after TNF-receptor complexes had formed. TNF-α enhanced kinase activity in a concentration-dependent manner at 5 min (Fig. 2B). TNF-α was effective at 10 pM and had a maximal effect at 3 nM; the ED_{50} was ≈300 pM TNF-α. This is similar to the ED_{50} of 200 pM for stimulation of ceramide-activated protein kinase by TNF-α in intact cells (*10*). TNF-α enhanced kinase activity in a total of 20 separate studies. Guanosine triphosphate (GTP) and guanosine-5′-*O*-(3-thiotriphos-

phate) (GTP-γ-S) (0.25 to 200 μM) did not affect kinase activity.

To demonstrate that the effect of TNF-α is mediated by sphingomyelin hydrolysis to ceramide, we added a sphingomyelinase or a phospholipase (A_2, C, or D) to the kinase reaction mixture and measured EGFR peptide phosphorylation. For some studies, the reaction mixture contained free Ca^{2+} (1 mM), which did not affect results. Control activity reflects several TNF-α–independent protein kinases that are known to phosphorylate EGFR peptide on Thr^{669}. Exposure of the nuclei-free supernates to sphingomyelinase (1×10^{-3} U ml^{-1}) from *Staphylococcus aureus* for 5 min induced an increase in kinase activity comparable to that induced by TNF-α (1 nM) (Fig. 3). This concentration of sphingomyelinase stimulates a twofold elevation in ceramide levels in HL-60 cells (*4, 13*). Concentrations of phospholipases A_2, C, and D, which were 40- to 400-fold higher than sphingomyelinase and which are effective for phospholipid hydrolysis under conditions used in these assays (*14*), did not enhance kinase activity. Hence, the effect of TNF-α in broken cell preparations was mimicked by a sphingomyelinase but not by other phospholipases.

The mechanism of coupling of the TNF receptor to sphingomyelinase is unknown. Neutral sphingomyelinase appears to be ubiquitous in mammalian cells and is externally oriented in the plasma membrane (*15*). Similarly, sphingomyelin is preferentially localized to the outer leaflet of the plasma membrane (*16*). This colocalization of receptor, phospholipase, and substrate at the plasma membrane suggests that ceramide is generated at this site. The exact intracellular site of the ceramide-activated protein kinase has not yet been investigated; however, preliminary evidence suggests it is an intrinsic membrane protein (*10*). In this regard, ceramide-activated protein kinase would not have to be present in the outer leaflet of the plasma membrane for signaling to occur, as ceramide can redistribute across a membrane bilayer (*17*).

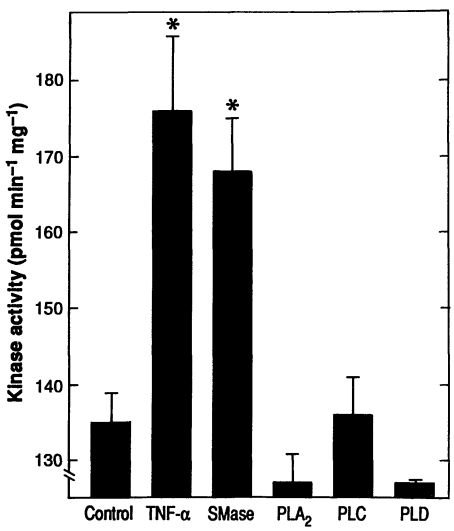

Fig. 3. Effect of phospholipases on ceramide-activated protein kinase activity. Nuclei-free supernates, prepared as in Fig. 1, were first incubated with TNF-α (3 nM) or added directly to reaction mixtures that contained various phospholipases: sphingomyelinase (SMase) (1×10^{-3} U ml^{-1}, *S. aureus*), phospholipase A_2 (PLA_2) (3.8×10^{-2} and 3.8×10^{-1} U ml^{-1}, *Vipera ruselli*), phospholipase C (PLC) (3.8×10^{-2} U ml^{-1}, *Bacillus cereus*), and phospholipase D (PLD) (3.8×10^{-2} U ml^{-1}, *Streptomyces chromofuscus*). Peptide phosphorylation was measured as in Fig. 2. Control value represents peptide phosphorylation in the absence of phospholipases or TNF-α. Values (mean ± SEM) represent data derived from duplicate samples in three experiments. *$P < 0.001$ compared to control.

It has been proposed that various distinct signaling systems, including protein kinases A and C, phospholipases A_2 and C, the EGFR tyrosine kinase, and a novel serine kinase, may mediate TNF-α action (*23*). It is clear that no single second messenger pathway can account for the entirety of the reported biologic effects of TNF-α. The role of the sphingomyelin pathway in events other than monocytic differentiation has not been investigated nor has the relation to these other signaling systems. This issue is further complicated by the recent cloning of two distinct TNF receptor forms of 55 kD and 75 kD (*24*) with homologous extracellular domains and dissimilar intracellular portions. HL-60 cells appear to contain both receptor forms (*25, 26*). Although no evidence exists to demonstrate which form activates the sphingomyelin pathway, the existence of activating and blocking receptor antibodies and cell lines containing a single receptor form (*25–27*) may allow for this distinction in the future.

In sum, the rapid kinetics of activation of the sphingomyelin pathway by TNF-α in intact cells, the ability of cell-permeable ceramide analogs to bypass receptor activation and mimic TNF-α action, and the reconstitution of this cascade in a cell-free system provide strong support for the notion that this pathway serves to couple TNF receptor activation to cellular stimulation. Hence, these studies suggest that TNF-α may activate a plasma membrane–bound neutral sphingomyelinase to generate the second messenger ceramide, which stimulates the ceramide-activated protein kinase to phosphorylate a distinct set of protein substrates, thereby altering their function.

REFERENCES AND NOTES

1. R. N. Kolesnick, *J. Biol. Chem.* **262**, 16759 (1987).
2. C. W. Slife *et al.*, *ibid.* **264**, 1 (1989).
3. Y. A. Hannun, C. R. Loomis, A. H. Merrill, Jr., R. M. Bell, *ibid.* **261**, 12604 (1986); A. H. Merrill *et al.*, *ibid.*, p. 12610; E. Wilson, M. Olcott, R. Bell, A. Merrill, Jr., D. Lambeth, *ibid.*, p. 12616.
4. K. A. Dressler and R. N. Kolesnick, *ibid.* **265**, 14917 (1990).
5. S. M. Bajjalieh, T. F. J. Martin, E. Floor, *ibid.* **264**, 14354 (1989); R. N. Kolesnick and M. R. Hemer, *ibid.* **265**, 18803 (1990).
6. R. N. Kolesnick, *Prog. Lipid Res.* **30**, 1 (1991).
7. T. Okazaki, R. M. Bell, Y. A. Hannun, *J. Biol. Chem.* **264**, 19076 (1990); T. Okazaki, A. Bielawska, R. M. Bell, Y. A. Hannun, *ibid.* **265**, 15823 (1990).
8. T. Goldkorn *et al.*, *ibid.* **266**, 16092 (1991).
9. M.-Y. Kim, C. Linardic, L. Obeid, Y. Hannun, *ibid.*, p. 484.
10. S. Mathias, K. A. Dressler, R. N. Kolesnick, *Proc. Natl. Acad. Sci. U.S.A.* **88**, 10009 (1991).
11. K. Imamura, M. L. Sherman, D. Spriggs, D. Kufe, *J. Biol. Chem.* **263**, 10247 (1988).
12. B. G. Rao and M. W. Spence, *J. Lipid Res.* **17**, 506 (1976).
13. R. N. Kolesnick, *J. Biol. Chem.* **264**, 7617 (1989).
14. _____, unpublished observations.
15. D. V. M. Das, H. W. Cook, M. W. Spence, *Biochim. Biophys. Acta* 777, 339 (1984).
16. Y. Barenholz and T. E. Thompson, *ibid.* **604**, 129 (1980).
17. N. G. Lipsky and R. E. Pagano, *Cell Biol.* **80**, 2608 (1983).
18. R. Seger *et al.*, *Proc. Natl. Acad. Sci. U.S.A.* **88**, 6142 (1991); T. G. Boulton *et al.*, *Science* **249**, 64 (1990); G. J. Heiserman and G. N. Gill, *J. Biol. Chem.* **263**, 13152 (1988).
19. I. C. Northwood, F. A. Gonzalez, M. Wartmann, D. L. Raden, R. J. Davis, *J. Biol. Chem.* **266**, 15266 (1991).
20. F. L. Hall *et al.*, *ibid.*, p. 17430.
21. E. Alvarez *et al.*, *ibid.*, p. 15277.
22. A. Aitken *et al.*, *Biochim. Biophys. Acta* **790**, 28 (1984).

23. J. Vilcek and T. H. Lee, *J. Biol. Chem.* **266**, 7313 (1991).
24. H. Loetscher *et al.*, *Cell* **61**, 351 (1990); T. Schall *et al.*, *ibid.*, p. 361; C. A. Smith *et al.*, *Science* **248**, 1019 (1990); Z. Dembic *et al.*, *Cytokine* **2**, 231 (1990).
25. M. Brockhaus *et al.*, *Proc. Natl. Acad. Sci. U.S.A.* **87**, 3127 (1990).
26. B. Thoma, M. Grell, K. Pfizenmaier, P. Scheurich, *J. Exp. Med.* **172**, 1019 (1990).
27. H. P. Hohmann, R. Remy, M. Brockhaus, A. P. G. M. van Loon, *J. Biol. Chem.* **264**, 14927 (1989); T. Espevik, M. Brockhaus, H. R. Loetscher, U. Nonstad, R. Shalaby, *J. Exp. Med.* **171**, 415 (1990); H. Engelmann *et al.*, *J. Biol. Chem.* **265**, 13397 (1990); B. Ryffel, M. Brockhaus, U. Durmuller, F. Gudat, *Am. J. Pathol.* **139**, 7 (1991).
28. K. A. Dressler, C.-C. Kan, R. N. Kolesnick, *J. Biol. Chem.* **266**, 11522 (1991); R. N. Kolesnick and S. Clegg, *ibid.* **263**, 6534 (1988).
29. J. Preiss *et al.*, *ibid.* **261**, 8597 (1986).
30. Supported by grants RO-1-CA-42385 from NIH and FRA-345 from the American Cancer Society (R.N.K.), National Research Service Award 1 F32 GM14207-01 (to K.A.D.), and the Charles A. Dana Foundation (K.A.D.). We thank L. Old and N. Rosen for comments.

7 November 1991; accepted 27 January 1992

Identification of the Integrin VLA-2 as a Receptor for Echovirus 1

JEFFREY M. BERGELSON,* MICHAEL P. SHEPLEY,† BOSCO M. C. CHAN,‡ MARTIN E. HEMLER, ROBERT W. FINBERG

Cell surface receptors for echovirus, a common human pathogen, were identified with monoclonal antibodies that protected susceptible cells from infection with echovirus 1. These monoclonal antibodies, which prevented virus attachment to specific receptor sites, recognized the α and β subunits of the integrin VLA-2 ($\alpha_2\beta_1$), a receptor for collagen and laminin. RD rhabdomyosarcoma cells expressed little VLA-2, did not bind to ^{35}S-labeled virus, and resisted infection until transfected with complementary DNA encoding the α_2 subunit of VLA-2. Thus, integrins, adhesion receptors important in interactions between cells and with the extracellular matrix, can mediate virus attachment and infection.

SPECIFIC RECEPTORS HAVE BEEN identified for only a few of the viruses that cause human disease (*1*). Echoviruses, nonenveloped RNA viruses belonging to the picornavirus family, are frequently responsible for febrile illness and viral meningitis (*2*). In newborn infants echoviruses can cause fatal disseminated infections (*2*). The integrin family of adhesion receptors is composed of at least 7 different β subunits and 14 different α subunits that associate to form at least 16 different heterodimers (*3*). Integrins mediate cell-to-cell interactions as well as cell interactions with the extracellular matrix and are involved in diverse functions such as cell migration, inflammation, and thrombus formation (*3–5*). VLA-2 ($\alpha_2\beta_1$) mediates cell attachment to collagen and laminin (*6*) and participates in tumor metastasis in vivo (*7*).

To identify cell surface proteins involved in echovirus attachment, we immunized mice with HeLa cells to obtain monoclonal antibodies (MAbs) capable of protecting cells from echovirus infection (*8*). Two protective MAbs, DE9 [immunoglobulin G1 (IgG1)] and AA10 (IgM), were obtained from independent hybridoma fusions. Binding of [^{35}S]methionine echovirus 1 was reduced by 90% when HeLa cell monolayers were first incubated with AA10, but this MAb did not inhibit binding of poliovirus 2 (Fig. 1A). DE9 reduced the binding of radiolabeled echovirus 1 by about 50%, but only when rabbit antibody to mouse immunoglobulin was added (Fig. 1B) (*9*).

Although both MAbs protected HeLa cells from the cytopathic effect of echovirus 1, they did not prevent cytopathic effects caused by other picornaviruses. AA10 protected cells from infection even at high multiplicity [100 plaque-forming units (PFU) per cell]. In addition, plaque formation by echovirus 1 was inhibited 100% when target monolayers were preincubated with AA10 (20 μg/ml): no plaques were seen when more than 100,000 PFU were added to AA10-treated monolayers. There was no comparable inhibition of plaque formation by other picornaviruses (Fig. 2). Incubation of echovirus directly with AA10 (20 μg/ml) did not reduce the viral titer, which indicates that the protective effect of AA10 resulted from its interaction with cells, not the virus.

Each MAb immunoprecipitated a pair of proteins (125 and 145 kD) from surface-radioiodinated HeLa cells under two detergent conditions (Fig. 3A). AA10 immunoprecipitated more of the larger protein. The molecular weights of the precipitated proteins resembled those reported for β_1 integrins (VLA proteins), which consist of a common 130-kD β_1 subunit in association with unique α subunits of 120 to 210 kD (*5*). Immunoprecipitation with DE9 and AA10 revealed the same protein patterns seen with Abs to the β_1 and α_2 integrin subunits of VLA-2 (Fig. 3B). Immunodepletion with a MAb to the β_1 subunit eliminated almost all material precipitable by DE9 (Fig. 3D). Depletion with AA10 itself

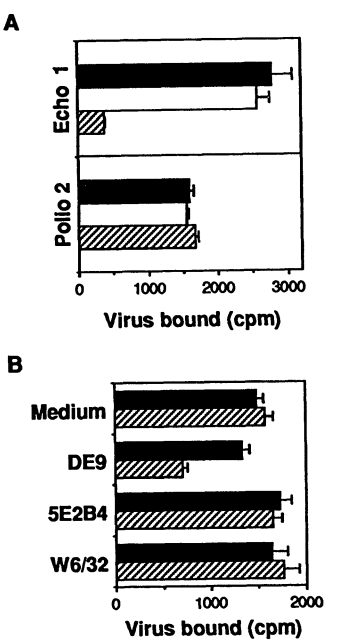

Fig. 1. Attachment of echovirus 1 to HeLa cell monolayers. Echovirus 1 and poliovirus 2w2 were labeled with [^{35}S]methionine and purified (*8*). Purity of the labeled virus was confirmed by electrophoresis in 12.5% polyacrylamide gels. (**A**) HeLa monolayers in 24-well tissue culture plates were first incubated for 30 min with MAbs (20 μg/ml) at room temperature, then washed and incubated for 30 min with the labeled virus (~20,000 cpm) in Hanks balanced salt solution containing 10 mM Hepes (pH 7.0), 20 mM $MgCl_2$, and 4% fetal calf serum. Dark bars, preincubated with medium; white bars, preincubated with control T9 (Coulter, Hialeah, Florida), an isotype-matched MAb to a HeLa cell surface antigen; hatched bars, preincubated with AA10. Radiolabeled virus bound per confluent monolayer (mean ± SD cpm bound for triplicate samples) is shown. Experiments were performed three times. (**B**) MAb-treated monolayers (dark bars) were washed and incubated with rabbit antibodies to mouse immunoglobulin (40 μg/ml; hatched bars) (Cappel, West Chester, Pennsylvania) for an additional 30 min before washing and addition of radiolabeled virus as in (A). 5E2B4 (*26*) recognizes the intracellular protein Tau. W6/32 (murine IgG2a, ATCC) recognizes a framework determinant of human major histocompatibility complex (MHC) class I, which is expressed on HeLa cells. Radiolabeled virus bound per confluent monolayer (mean ± SD cpm for four samples) is shown. In control experiments, DE9 did not inhibit binding of poliovirus 2, whether or not second antibody was used.

J. M. Bergelson, M. P. Shepley, R. W. Finberg, Laboratory of Infectious Disease, Dana-Farber Cancer Institute, Harvard Medical School, Boston, MA 02115.
B. M. C. Chan and M. E. Hemler, Division of Tumor Virology, Dana-Farber Cancer Institute, Boston, MA 02115.

*To whom correspondence should be addressed.
†Present address: Department of Microbiology, Columbia University College of Physicians and Surgeons, New York, NY 10032.
‡Present address: Department of Chemistry and Biochemistry, University of Guelph, Guelph, Ontario, NIG 2W1, Canada.